C. R. Physique 3 (2002) 1277–1292

Physique appliquée/*Applied physics*

MÉCANISMES PHYSIQUES DU NUAGE D'ORAGE ET DE L'ÉCLAIR

THE PHYSICS OF THUNDERCLOUD AND LIGHTNING DISCHARGE

The physical origin of the land–ocean contrast in lightning activity

Earle Williams [a], Sharon Stanfill [b]

[a] Parsons Laboratory, MIT, Cambridge, MA 02139, USA

[b] MIT Lincoln Laboratory, Lexington, MA 02173, USA

Note presented by Guy Laval.

Abstract New tests and older ideas are explored to understand the origin of the pronounced contrast in lightning between land and sea. The behavior of islands as miniature continents with variable area supports the traditional thermal hypothesis over the aerosol hypothesis for lightning control. The substantial land–ocean contrast in updraft strength is supported globally by TRMM (Tropical Rainfall Measuring Mission) radar comparisons of mixed phase radar reflectivity. The land–ocean updraft contrast is grossly inconsistent with the land–ocean contrast in CAPE (Convective Available Potential Energy), from the standpoint of parcel theory. This inconsistency is resolved by the scaling of buoyant parcel size with cloud base height, as suggested by earlier investigators. Strongly electrified continental convection is then favored by a larger surface Bowen ratio, and by larger, more strongly buoyant boundary layer parcels which more efficiently transform CAPE to kinetic energy of the updraft in the moist stage of conditional instability. ***To cite this article: E. Williams, S. Stanfill, C. R. Physique 3 (2002) 1277–1292.***

aerosol / convection / islands / lightning / thermals / thunderstorm / updrafts

Origine physique du contraste entre activité électrique au dessus des terres et des océans

Résumé L'origine du contraste prononcé entre activité électrique au dessus des terres et des océans est explorée à l'aide de concepts classiques et de nouvelles méthodes d'analyse. Le comportement des îles, considérées comme similaires à des continents miniatures, est en faveur d'un contrôle de l'activité électrique par un mécanisme thermodynamique plutôt que par la présence d'aérosols. L'activité électrique au-dessus des îles, considérées comme similaires à des continents miniatures, est pilotée par un mécanisme thermodynamique plutôt que par la présence d'aérosols. Les mesures de réflectivité radar dans le cadre de la mission TRMM (Tropical Rainfall Measuring Mission) soulignent le contraste important entre l'intensité des ascendances mesurées au dessus des terres et des océans. Cependant, ce contraste en termes d'ascendance ne peut pas être attribué à une différence d'instabilité convective potentielle (CAPE) déterminée en référence à la flottabilité des masses d'air. Ce problème est résolu en dimensionnant celles-ci selon l'altitude de la base du nuage, comme cela avait été suggéré lors d'études précédentes. Une convection continentale associée à une forte activité électrique est donc favorisée par un rapport de Bowen surfacique plus important et par une plus grande instabilité convective en couche limite. Ceci conduit à une transformation plus efficace de l'instabilité convective potentielle en énergie cinétique

E-mail address: earlew@ll.mit.edu (E. Williams).

S1631-0705(02)01407-X/REV

des courants ascendants nuageux. ***Pour citer cet article : E. Williams, S. Stanfill, C. R. Physique 3 (2002) 1277–1292.***

aérosols / convection / foudre / thermique / orages / ascendances

1. Introduction

The first quantitative evidence for a large contrast in lightning activity between land and sea is found in the analysis of station thunder days [1] on a global basis. These results revealed a 5–10 fold land–ocean contrast in the percentage of days in a year when thunder is heard. This analysis played a pivotal early role in the formulation of the global electrical circuit following C.T.R. Wilson's hypothesis that thunderstorms are the global circuit source. Brooks' results were needed in the interpretation of the integrated measurements of electric potential gradient [2] – the so-called 'Carnegie Curve'. The mismatch in the UT amplitude variation of the Carnegie curve and Brooks' thunder day observations led to speculation that oceanic thunderstorms were not properly represented due to the sampling limitations [2,3]. Global lightning observations in the modern satellite era, first at local midnight [4], and later over the entire diurnal cycle [5] as a highlight of the NASA Tropical Rainfall Measuring Mission (Fig. 1), now clearly corroborate Brooks' analysis [1], showing an order of magnitude land–ocean contrast. These findings thereby require an alternative explanation for the mismatch in amplitude variation between the Carnegie curve and any measure of the UT variation of global lightning activity [6].

The traditional explanation for this now firmly established dominance of continental lightning is based on the contrast in surface properties. The land surface with its lower heat capacity and immobile nature, whether it be rock, soil, or vegetation, heats more readily than seawater. In terms of fluxes of sensible and latent heat, the turbulent flux of sensible heat is relatively enhanced over continental surfaces, and the Bowen ratio for land is systematically greater than for sea. The land surface is systematically hotter and hence the lower atmosphere is more unstable to vertical air motions which are vital to deep convection, the thunderstorm ice factory, electric charge separation, and lightning. One oft-used measure for the vertical velocity based on parcel theory is Convective Available Potential Energy (CAPE). Well established positive

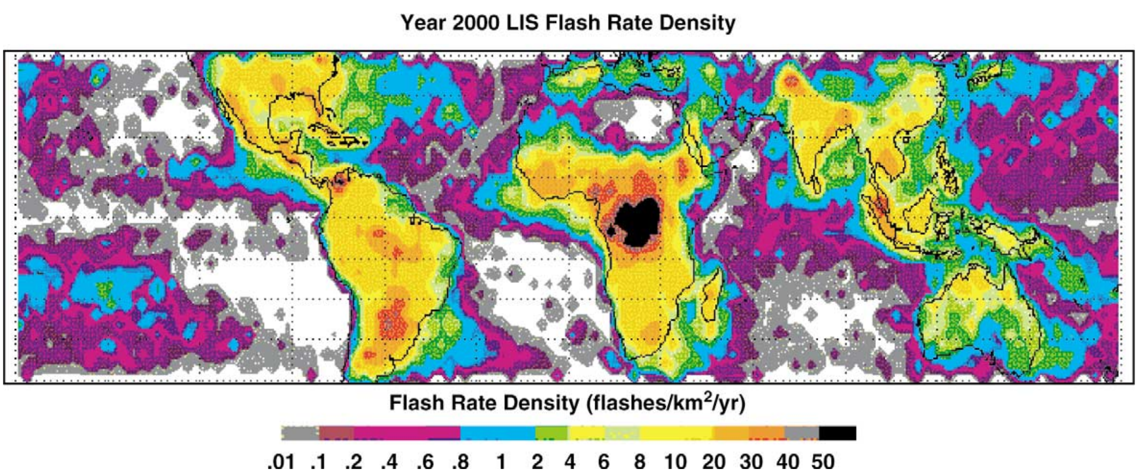

Figure 1. Global lightning map based on three years of observations from the NASA TRMM Lightning Imaging Sensor [52] illustrating the order-of-magnitude land–ocean contrast, and the ranking of the three tropical 'chimney' regions.

correlations between CAPE and the wet bulb potential temperature of surface air [7] for land and ocean alike, form the basis for the hypothesis for the response of the global electrical circuit to temperature [8–14]. A recent study [15] has shown evidence for this correlated relationship on decadal time scales.

Over the last decade, one substantial weakness has been identified with the so-called thermal hypothesis for the land–ocean lightning contrast. Measurements of CAPE over land and warm ocean regions show little contrast [7,16]. The maximum wet bulb potential temperature is systematically higher over land than over sea [7], but this comparison is misleading because the upper air temperature is also greater over land, thereby supporting some degree of convective adjustment and an equalization of CAPE.

Furthermore, the suggestion that the 'shape of the CAPE' (the distribution of cloud buoyancy with altitude) might explain regional differences in tropical lightning has not met with much success [17].

Meanwhile, an alternative hypothesis for the land–ocean lightning contrast has developed, based on a well established contrast in boundary layer aerosol concentration (and resulting electrical conductivity of the air) between land and sea (D. Rosenfeld, personal communication, 1998). Global variations in cloud droplet size have also been observed which are broadly consistent with the land–ocean contrast in cloud condensation nuclei concentrations [18]. Although recent tests of this hypothesis in the lightning context in a field experiments in Brazil [19] cast doubt on a primary role for aerosol, questions remain about why this mechanism is not operating as hypothesized. A recent study [20] has suggested a role for aerosol in explaining the local enhancement in lightning in the vicinity of Houston, Texas where an abundance of aerosol is well documented.

This study is concerned with a critical reexamination of both the thermal and the aerosol hypotheses. This reexamination will include a consideration of lightning over islands (Section 2), the occurrence of strong mixed phase development (Section 3) and warm precipitating clouds over land and sea (Section 4), and a revisitation of the validity of parcel theory which heretofore has been a mainstay of the thermal hypothesis (Section 5). The results will show that the thermal hypothesis and conditional instability remain viable, but that other thermodynamic differences between land and sea need to be considered. The results will also point to an important role for both dry bulb and wet bulb potential temperature in influencing global lightning activity.

2. The dependence of lightning activity on island area

The continental dominance of lightning activity is well established. Islands are miniature continents. How large an island area is required to guarantee continental behavior in the realm of cloud electrification and lightning? Fortunately, the answer to this question is dependent on the hypothesized physical origin of the continental electrification. The treatment of islands as thermal perturbations and as boundary layer aerosol perturbations leads to very different predictions for critical island area.

An island acting as a thermal perturbation is illustrated in Fig. 2, where R is the radius of a circular island and h is the boundary layer thickness. The larger Bowen ratio of the island surface compared to the adjacent ocean leads to differential heating of the island boundary layer by sunlight, lending buoyancy to the surface air. This air rises to form the cloud and ultimately the updraft w. For a fixed cloud radius r, the upward flux is $\pi r^2 w$ ($\mathrm{m^3 \cdot s^{-1}}$). If the cloud lifetime is τ, the total volume of air drawn upward is $\pi r^2 w\tau$. This volume is drawn entirely from the boundary layer, requiring:

$$\pi R^2 h = \pi r^2 w\tau.$$

Or the area from which the boundary layer air is drawn is

$$\pi R^2 = \pi \frac{w\tau}{h} r^2.$$

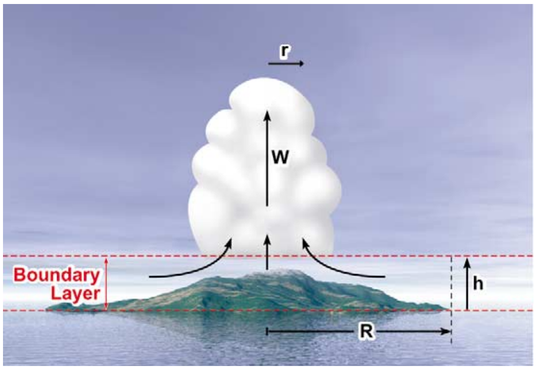

Figure 2. Illustration of convective inducement by an island, following the thermal hypothesis for the land–ocean lightning contrast.

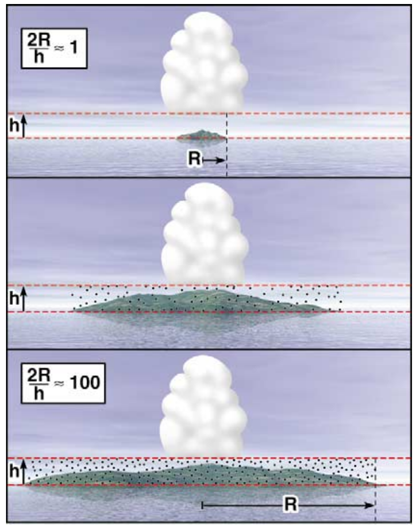

Figure 3. Illustration of aerosol perturbation of island convection, following the aerosol hypothesis for the land–ocean lightning contrast.

If this area exceeds the island area, then colder oceanic air is entrained and the island's thermal budget is diluted. In general, the scaling parameters are not independent, and both w and τ will increase with cloud size [21,22]. Inserting representative values [21–24] for quantities ($w = 5$ m·s^{-1}, $h = 500$ m, $r = 1000$ m and $\tau = 3600$ s) gives a critical island area, $\pi R^2 \approx 110$ km^2. Convection over islands with substantially smaller areas will not find sufficient continental air to feed upon and is expected to retain maritime characteristics.

The island aerosol perturbation is illustrated in Fig. 3. In this context, the important scales in the problem are island diameter and the polluted boundary layer thickness. A crude preliminary estimate for critical island size necessary for continental behavior would require that the island diameter be large in comparison with h, say $2R/h > 100$. This condition leads to a critical island area of:

$$\pi\left(\frac{100h}{2}\right)^2 \approx 20\,000\ \mathrm{km}^2.$$

An alternative and improved way to estimate a critical island size recognizes the role of the intruding sea breeze front in replacing the island's polluted boundary layer with cleaner maritime air. If the area 'cleaned' in this way in half a day is less than the island area, then the island would be considered 'continental'. Observations of the sea breeze progression over the Florida peninsula indicate that approximately half a day is required for sea breezes from opposite coasts to 'meet' at mid-peninsula. On this basis, we can take half the peninsula width (100 km) as a measure of critical island radius R. This gives:

$$\pi R^2 = \pi(100\ \mathrm{km})^2 \approx 30\,000\ \mathrm{km}^2.$$

Happily, this estimate for critical island area for continental aerosol control is of the same order as the cruder estimate. Furthermore, both estimates are larger (by more than two orders of magnitude) than the critical area for thermal perturbation.

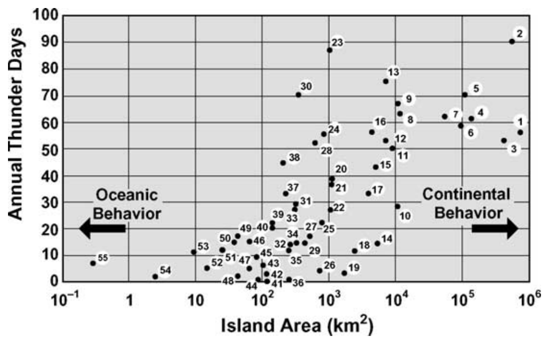

Figure 4. Annual number of thunder days [25] for islands versus island area.

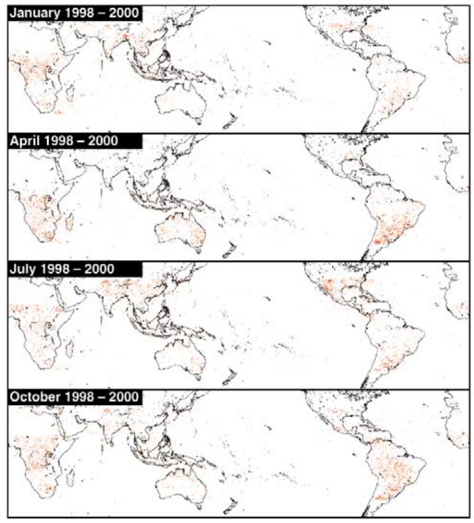

Figure 5. Global maps of all locations showing radar echoes at 7 km altitude with reflectivity greater than or equal to 40 dBZ based on observations with the TRMM precipitation radar in space. Maps for three Januarys, three Aprils, three Julys and three Octobers in the period 1997–2000 are shown.

As a quantitative test of these predictions, annual thunder day counts for all islands included in the WMO worldwide compilation [25] have been examined. The corresponding island areas were extracted from the UNEP (United Nations Environmental Program) web site. These results are listed in Table 1 by island (in order of increasing island area) and plotted in Fig. 4. When multiple station observations are available for an island, the largest annual thunder day count is taken to represent that island. Unfortunately, only three islands smaller than 10 km^2 are available with accompanying thunder day information, so the oceanic limit is rather sparsely represented. Despite considerable scatter overall, Fig. 4 does show clear evidence for a transitional area in the range of 10^2–10^3 km^2 between oceanic and continental thunder day behavior. This result is decidedly closer to the prediction for a thermal perturbation (110 km^2) than an aerosol perturbation (20–30 000 km^2), and so supports the traditional hypothesis for the land–ocean lightning contrast.

3. The land–ocean contrast in elevated cores of strong radar reflectivity

The strong empirical relationship between the vertical development of radar reflectivity in the mixed phase region of moist convection and the attendant lightning activity has been emphasized in numerous field studies (see numerous references in [26]). Simple scaling relationships [27] and modeling studies [28,29] have focused on the central role of the updraft in shaping the vertical profile of radar reflectivity and in invigorating the ice phase microphysics favorable to active lightning. Ongoing observations with the TRMM satellite enable global mapping of mixed phase radar reflectivity with a single instrument to examine the land–ocean lightning contrast. This satellite is in a low earth orbit (350 km altitude) and circles the earth every 90 minutes. With each orbit, a 215 km-wide swath of downward pointing radar observations is carried out with a horizontal resolution of 4 km (one pixel size is nominally 4 km $\times$ 4 km) and a vertical resolution of 250 meters. For purposes of the land–ocean comparison, every orbit for the 3-year period 1998–2000 was queried for all geographical locations of radar echoes (isolated pixels) at a fixed 7.0 km MSL altitude (within the mixed phase region of moist convection) with reflectivity factor equal

Table 1. Tabulation of islands, areas, maximum elevations and annual thunder day counts.

	Island name	Area (km^2)	Elevation (m)	Thunder days
1	Borneo	748 000	4175	56
2	Madagascar	587 713	2876	90
3	Sumatra	443 000	3804	53
4	Java	139 000	3676	61
5	Luzon	110 000	2934	71
6	Mindanao	97 530	2954	59
7	Sri Lanka	67 654	2524	62
8	Panay	12 011	2049	63
9	Jamaica	11 189	2256	67
10	Suva	10 531	1224	28
11	Puerto Rico	9099	1338	50
12	New Ireland	7404	2150	53
13	Leyte	7367	1349	75
14	Bali	5416	2276	14
15	Trinidad	5008	940	43
16	Cebu	4467	1097	56
17	Espiritu Santo	3955	1879	33
18	Reunion	2535	3069	11
19	Mauritius	1873	828	3
20	Martinique	1167	1397	39
21	Upolu	1125	1143	38
22	Tahiti	1069	2241	27
23	Grande Comore	1012	2361	87
24	Jolo	868	812	55
25	Ambon	805	1031	22
26	Madeira	749	1861	4
27	St. Lucia	639	950	17
28	Guadaloupe	639	136	52
29	Barbados	462	340	15
30	Mayotte	371	660	70
31	Ponape	334	791	29
32	Grenada	323	840	15
33	Tobago	309	576	27
34	Antigua	277	402	14
35	Niue	264	73	12
36	Sao Vicente	233	743	1

Table 1. Continued.

37	New Providence	228	?	33
38	Virgin Islands	214	355	45
39	Danger	150	?	22
40	Mahe	148	905	20
41	Ste Helen	125	819	0
42	Montserrat	124	915	3
43	Vavau	103	204	6
44	Ascension	125	819	0
45	Eua	86.7	328	9
46	Rarotonga	67.6	653	15
47	Gough	66.6	910	5
48	Rotuma	44	256	2
49	Bermuda	39	79	17
50	Pitcairn	37.3	33	16
51	Desirade	27	?	12
52	Ocean	15	?	5
53	Penrhyn	9.8	?	11
54	Cargados	2.7	?	2
55	Agalega	0.3	?	7

to or greater than 40 dBZ. This condition is frequently associated with lightning activity. Maps showing all such locations for (1) three Januarys, (2) three Aprils, (3) three Julys, and (4) three Octobers, are shown in Fig. 5. The land–ocean contrast is dramatic, with the great majority of locations over land. Broad (4 km) updrafts with strong reflectivity aloft are a rare phenomenon over oceans. The few cases over water tend to be located in the western ocean basins, where warm ocean currents flow poleward beneath cold surface air. Also apparent in Fig. 5 is the seasonal latitudinal migration of the strongly developed convection over land, most apparent over South America and Africa.

4. The land–ocean contrast in 'warm' rain production

An essential aspect of the aerosol hypothesis [19] is the role of cloud condensation nuclei in controlling the cloud droplet size. The contrast in CCN between land and ocean is estimated in Table 2. When boundary layer air is polluted as is the case generally over continents, the cloud droplets are more numerous but smaller in size, thereby suppressing coalescence and the production of 'warm' rain. By contrast, when the air is clean as is the case generally over oceans [30], the adiabatic cloud water is shared among a smaller number of cloud droplets. As a consequence, the individual droplets are larger and coalescence is enhanced, thereby promoting 'warm rain'. One qualitative prediction of the aerosol hypothesis then is that warm rain clouds will be plentiful over oceans and sparse over continents.

Observations of warm precipitating clouds with the TRMM radar in space also enable a test of this prediction. For purposes of the present study, every TRMM orbit for the 3-year period 1998–2000 was queried for geographical locations of radar echoes (isolated pixels) with reflectivity in excess of the radar sensitivity (18 dBZ), and simultaneously confined to altitudes less than the height of the 0 °C isotherm

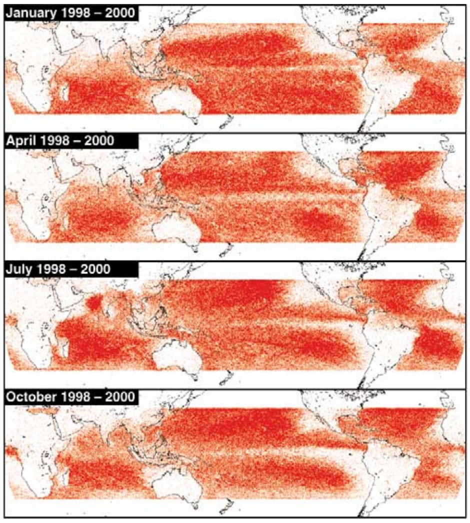

Figure 6. Global maps of all locations showing isolated 'warm' precipitation echoes based on observations with the TRMM precipitation radar in space. Maps for three Januarys, three Aprils, three Julys and three Octobers in the period 1997–2000 are shown.

(chosen here to be 5 km MSL). Maps showing the locations of all such isolated warm rain locations for (1) three Januarys, (2) three Aprils, (3) three Julys, and (4) three Octobers, are shown in Fig. 6.

Consistent with the qualitative predictions of the aerosol hypothesis, all maps show a great preponderance of warm rain clouds over oceans, with clear avoidance over land areas. On a per-unit-area basis, the contrast is cloud counts exceeds an order of magnitude. One can also readily perceive zonal bands sparse in warm rain, as well as sparse regions in the eastern oceans, likely associated with colder ocean water.

The traditional thermal hypothesis for the land–ocean lightning contrast also carries with it a qualitative prediction for the land–ocean contrast in warm rain production, which leaves the overall interpretation of Fig. 6 ambiguous. Following the work of [31] and others, the larger updrafts over continents (both in the dry boundary layer air and at higher levels in moist convection) will allow less time for droplets to interact for coalescence, and may therefore forestall the formation of warm rain. This action may effectively move the location of initial radar echo to the cold (sub-freezing) part of the atmosphere, in comparison with the situation over the ocean. The maps in Fig. 6 are therefore also qualitatively consistent with the thermal hypothesis. The contrast in updraft strength between land and ocean, strongly supported by the global maps in Fig. 5, is a particularly important basis for the discussion in the following section.

5. Revisitation of the traditional thermal hypothesis

The main thesis of this paper upholds the traditional thermal hypothesis based on conditional instability, but invokes inaccuracies in parcel theory to account for the pronounced land–ocean contrast. Several authors [32–34] have also speculated on this explanation. The arguments in support of this thesis depend on a contrast in certain physical parameters between land and ocean, summarized in Table 2.

Considerable evidence that parcel theory is inaccurate has long been recognized. The most obvious evidence is encountered early in the daytime during the incipient stage of moist convection when cloud parcels are smallest and hence most susceptible to mixing with drier environmental air. As pointed out in [7], it is common experience in the tropical atmosphere for the presence of widespread CAPE but with few, if any, deep cumulonimbi. The 'condition' of conditional instability (lifting of surface parcels to the LCL, formation of cloud, development of buoyancy) is very frequently satisfied, but the ensuing moist buoyant ascent to the level of neutral buoyancy is very rare. Small cloudy parcels simply do not survive the mixing process and become 'fossils' with no further growth. No particular emphasis has been given to land–ocean differences in behavior at this stage of convection, though earlier analyses of fair weather cumuli do show evidence for larger cloud diameters over land than over sea [35].

Table 2. Land–ocean contrast in key physical parameters.

Parameter	Land	Ocean
CCN Concentration (per cm^3)	>1000	100–200
Surface relative humidity (%)	20–60	80
Cloud base height (m)	1000–4000	500
$T_S - T_A$ (°C)	1–10	<1
Median cloud base updraft speed ($m \cdot s^{-1}$)	5	2
CAPE ($J \cdot kg^{-1}$)	0–3000	0–3000
Bowen ratio (sensible/latent)	0.2–1	0.1

The evidence for a failure of parcel theory at a more mature stage of convection (when buoyant parcels are substantially larger) is more subtle because simultaneous observations of CAPE and updraft speed W are scarce. However, numerous observations of CAPE [7,16] and updraft speed are available for land and ocean convection that enable a statistical quantification of the inaccuracy of parcel theory for the land–ocean contrast. According to parcel theory, if CAPE is efficiently converted to kinetic energy of updraft, the maximum updraft speed is

$$W_{max} = \sqrt{2\ \mathrm{CAPE}}.$$

The land–ocean updraft contrast can then be computed as:

$$\frac{W_{land}}{W_{ocean}} = \sqrt{\frac{\mathrm{CAPE}_{land}}{\mathrm{CAPE}_{ocean}}}.$$

As indicated in Table 2, measurements of updraft speed in cumulonimbi show a land–ocean ratio greater than two, thereby requiring a land–ocean CAPE ratio greater than four. This prediction is not consistent with any measurements. Most CAPE comparisons [7] show land–ocean differences of at most 50%. One study [16] presents evidence that the CAPE ratio is of order unity, when warm ocean regions are considered. This discrepancy between theory and measurement is a fundamental problem and a major incentive for further study.

Conditional instability is a two-stage process – a dry stage in the planetary boundary layer and a subsequent moist stage above cloud base. Air is required to rise in the dry stage to provide the ‘condition’ (i.e., condensation and provision of cloud buoyancy by latent heat release) for conditional instability. In many previous studies of deep convection [19,27,36,17], the dry stage has received scant attention because parcel size was given no importance. The moist stage and the associated wet bulb potential temperature have been emphasized in these studies rather than the dry bulb temperature appropriate for the dry stage of convection.

The contrast in boundary layer parameters between land and ocean in Table 2 serve as a reminder that these differences may be important, and furthermore may have important implications for the subsequent moist component of conditional instability. The contrast in boundary layer thermal speeds between land and ocean is widely recognized [37]. The air-sea temperature contrast [38] is typically less than 1 °C, in marked contrast with differences over land, and this difference in dry buoyancy is the accepted explanation for the contrast in thermal speeds. It is also important to point out that because dry thermal buoyancy is controlled primarily by dry bulb temperature (and its contrast with the local environment), the largest updrafts will be achieved if all sunlight is invested in sensible heat and none in evaporation. The Bowen ratio is also contrasted for land and ocean in Table 2.

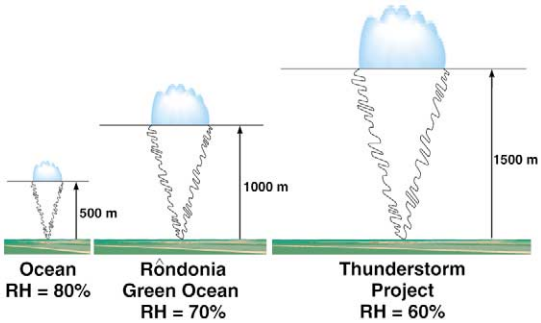

Figure 7. Illustration that thermal width and moist convective updraft width scale with the height of cloud base. The scale-independent angle of plume expansion in the vertical is based on similarity theory and supported by laboratory scale experiments with buoyant plumes.

The implications for this contrast in physical parameters for the dry stage of convection and the incipient moist convection are illustrated schematically in Fig. 7. As discussed in [39], the cloud base height is closely related to boundary layer relative humidity also summarized in Table 2. Over the oceans, the relative humidity is 80% and the tropical cloud base height is only 500 m. In increasingly continental conditions of larger Bowen ratio and lower relative humidity, the cloud base is systematically higher. In extreme desert scenarios, cloud may never form.

Both theory and observation support the concept that boundary layer thermals are not only stronger, but also broader, in more continental conditions. Similarity theory for point sources of buoyancy in fluids show conical expansion of turbulent thermals with a fixed angle ($\sim 10^{\circ}$) with respect to the vertical for a wide variety of conditions [40]. The monotonic broadening with altitude guarantees that the widths of thermals will be greater, on average, at cloud base height when the cloud base is also higher. Sailplane measurements [41] provide evidence that thermals are systematically wider in deeper boundary layers, also supporting the scaling evidence in Fig. 7.

The picture in Fig. 7 is a highly simplified representation of real boundary layer behavior. More recent laboratory experiments [42] suggest departures from the self-similar behavior illustrated here when the thermal source width is appreciable compared to the thermal height. However, the sailplane evidence for scaling with cloud base height [41] does provide the basis for some testable predictions for the moist stage of deeper convection. Namely, the updraft widths of oceanic cumulonimbi are expected to be consistently smaller than continental updrafts. Fig. 8 presents observations of updraft widths for GATE (Global Atlantic Tropical Experiment) over the tropical Atlantic Ocean [24], from the Thunderstorm Project in Florida and Ohio [20], and from large hailstorms in Colorado [43]. The mean widths for continental thunderstorms are more than double the oceanic widths, broadly consistent with the scaling picture in Fig. 7, and also consistent with the global maps of 4 km-wide reflectivity cores in Fig. 4.

The very large continental thunderstorms with the largest updraft widths (occasionally, an order of magnitude greater than their oceanic counterparts) stand at the opposite extreme. With cloud water contents that come closest to adiabatic [44] and with updraft velocities that are more accurately predicted from parcel theory (references in [26]), these storms appear to achieve the undilute ascent that had been postulated earlier for tropical 'hot towers' [45].

The contrast in updraft speed between land and ocean cumulonimbi has already been discussed, but one final comparison in light of Fig. 7 is worth making. A summary of the land–ocean contrast in updraft profile [31] is reproduced in Fig. 9. The updraft contrast is greatest high in the cloud in the moist stage, but even at cloud base height, a factor-of-two contrast is evident. This finding lends further support to an important control from the dry boundary layer in influencing subsequent development. This observation may have fundamental importance in explaining the global maps of warm precipitating clouds shown in Fig. 6 in the previous section of this paper.

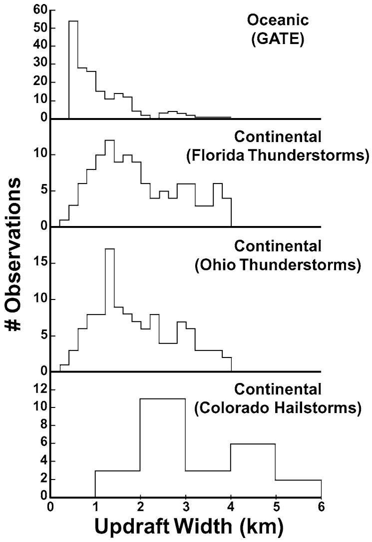

Figure 8. Histograms of observations of updraft width in: (a) oceanic conditions [24]; (b) Florida thunderstorms [23]; (c) Ohio thunderstorms [23]; and (d) large Colorado hailstorms [43].

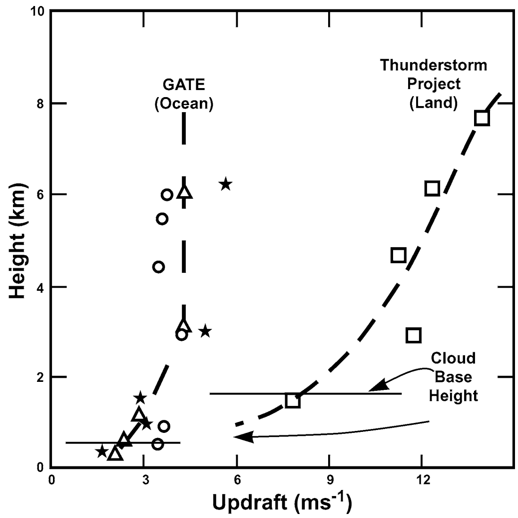

Figure 9. Summary of updraft profiles for oceanic and continental conditions [31]. The contrast in updraft strength exceeds a factor of two even at cloud base height.

6. Land–ocean contrasts in surface characteristics

In tests of the aerosol hypothesis for cloud electrification in Brazil [19], observations revealed a pronounced maritime regime during the wet season dubbed the ‘green ocean’. Given the skepticism raised in that study about a primary role for aerosol, and the accumulated evidence in favor of the traditional thermal hypothesis in the present study, it is appropriate to revisit this ocean-like regime over land. Characterized in the atmosphere by extensive warm rain production, weak radar reflectivity in the mixed phase region of deep convection, and by little if any lightning, and in the ground by water-saturated conditions and peak river discharge, this regime comes as close as possible to ocean conditions over continent.

The same study [19] also contrasted the ‘green ocean’ regime with the highly electrified conditions in the wet-to-dry season transition, also called ‘premonsoon’. The latter regime exhibited twice as many cloud-to-ground discharges, higher peak flash rates by a factor of 2–5, and larger lightning yield per unit rainfall than during the wet season. Comparisons of CAPE between these two regimes (based on the analysis of soundings from other years) however showed a negligible difference in mean values, a situation parallel with the present land–ocean CAPE comparisons.

Analysis of the Bowen ratio (BR) over South America [46] enables a comparison of surface characteristics in the wet season months (Jan–Mar) and the premonsoon months (Sep–Nov) for Rondonia, Brazil, shown in Figs. 10 (a) and (b). The wet season map (Fig. 9(a)) shows extensive regions of $BR < 0.25$ over the entire continent, and very prominently over Rondonia. (Also included in Table 1 are Bowen ratio estimates for land and ocean surfaces.) Undoubtedly, a map pertaining to only the ‘green ocean’ regime within the wet season would show even greater departures from continental behavior. In the premonsoon (Fig. 10(b)), in advance of the heavy rain, the ground is drier and the *BR* is larger by a factor-of-two in the Rondonia region, with the wetter conditions with attendant smaller *BR* displaced to the north.

Surface comparisons of this nature may be extended to global scale in attempts to account for the gross features of global lightning shown in Fig. 1. With improvements in the measurement of global lightning, the ordering of the three major tropical chimney zones has come into sharper focus. In both total lightning flash count and in flash density, the Maritime Continent shows least activity, like the oceans for which it is

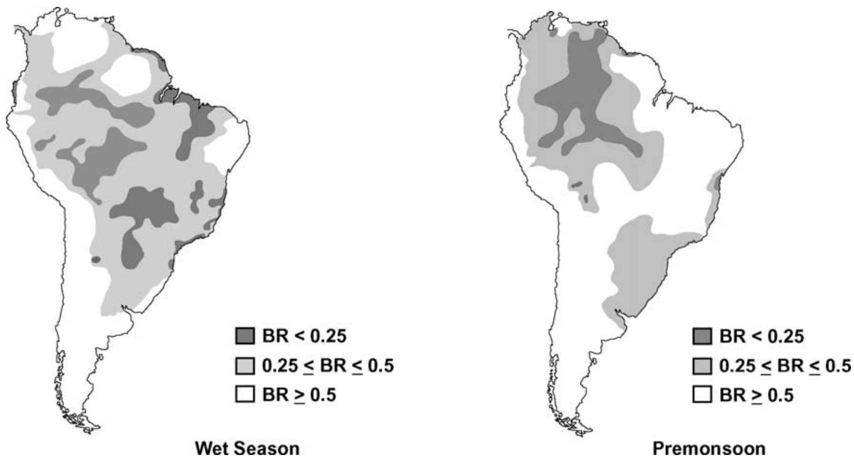

(a) (b)

Figure 10. Maps of Bowen ratio (*BR* = ratio of sensible to latent heat flux) for South America, for: (a) the wet season months; and (b) the premonsoon months for Rondonia, Brazil. Adapted from [46].

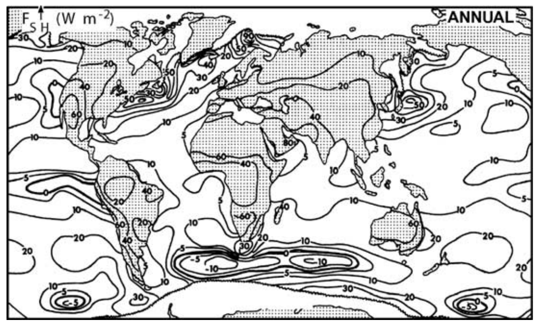

Figure 11. Global map of sensible heat flux at the surface for the year [47]. The units are watts per square meter.

named. The ‘green ocean’ of South America ranks second, and Africa, the most continental ‘chimney’, is the clear winner, with roughly twice the peak flash density and total lightning observed in South America. This overall behavior is mirrored by the annual map of sensible heat flux [47], reproduced in Fig. 11. The desert conditions in subtropical Africa with extraordinarily large values are widely recognized, but even in the heart of the Congo River basin (where lightning activity in Fig. 1 shows a clear maximum), the sensible heat flux is twice as large as in the Amazon basin in Brazil. Also consistent with Fig. 1, the sensible heat flux in South America is roughly twice that over the Maritime Continent.

7. Discussion

New tests aimed at clarifying the physical basis for the land–ocean lightning contrast tend to support the traditional thermal hypothesis. The island study shows a transitional island area more consistent with the thermal hypothesis than the aerosol hypothesis (Fig. 4). The pronounced contrast in elevated 40 dBZ locations (Fig. 5) is consistent with a land–ocean contrast in updraft strength identified in Thunderstorm Project/GATE comparisons more than twenty years ago. The empirical relationship linking updraft strength and mixed phase reflectivity development with lightning activity is widely documented. The closer examination of conditional instability, showing evidence for a scaling of parcel size with cloud base height, brings resolution to a long-standing paradox: the land–ocean contrast in updraft strength is substantial but the land–ocean contrast in CAPE is not. Recent modeling results [48] on deep convection substantiate a role of cloud base height in regulating updraft speeds by controlling parcel size. Recent satellite comparisons between land and ocean show evidence for greater supercooled water contents in continental clouds [49], also consistent with suppressed mixing in broader updrafts.

The aerosol hypothesis [19] has its own explanation for the land–ocean updraft contrast. This explanation involves the additional latent heat of freezing available when smaller droplets, more immune to coalescence to produce warm rain at lower levels, attain the mixed phase region. The weight of the evidence presented in this study shows an important role for parcel buoyancy in the dry part of the atmosphere in promoting stronger updrafts at higher levels. This explanation relies completely on the land–ocean contrast in surface properties (Table 2) and is completely independent of any contrast in aerosol. The substantial land–ocean contrast in updraft strength at cloud base height (Fig. 9) is not easily explained by the aerosol hypothesis.

The predominance of warm rain over oceans (Fig. 6) is qualitatively consistent with both the thermal and the aerosol hypotheses. Weaker updrafts and smaller CCN concentrations will both contribute to warm rain formation. Further quantitative resolution of the roles of updraft and CCN concentration will require detailed microphysical modeling with accurate collision/coalescence physics versus droplet size. Such calculations are currently underway (D. Rosenfeld and A. Khain, personal communication, 2002).

The postulated cloud-base-height influence on deep convection illustrated in Fig. 7 and supported by the results on updraft width in Fig. 8 has a point of diminishing return. As the surface becomes drier, and the Bowen ratio increases, and the relative humidity drops and the dry thermal buoyancy increases, and the cloud base height rises, the availability of sufficient moisture to support a thunderstorm becomes an issue. In desert environments with relative humidity at 20% or less, the theoretical cloud base height may be so high that cloud formation is prevented entirely. The optimal condition for cloud electrification however may exist in the range of 50–60% relative humidity with associated cloud base heights of 2000–3000 meters [39]. Perhaps not fortuitously, this range includes the giant supercell storms in the lee of the Rocky Mountains, which produce the largest hail and which are likely the most electrically active on the planet [26]. These storms are also the ones for which simple parcel theory predictions for updraft strength based on CAPE are most accurate.

The results of this study also have several implications for the earlier idea that global lightning is responsive to global temperature [8–14].

(i) Early investigations of global circuit response to temperature [7,8,11,13] emphasized dry bulb temperature, the traditional measure of global warming. More recent studies have focused on wet bulb potential temperature [9,10,50], largely because of the connection between the moist phase of conditional instability and the physical process of charge separation, and because of empirical evidence that CAPE and wet bulb temperature are roughly linearly related on short time scales [7]. The present study redirects attention to the importance of dry bulb temperature, in its effect on parcel buoyancy in the dry phase that subsequently impacts the moist phase. The main thesis here is that land lightning dominates over ocean lightning because land is hotter, in a dry bulb sense. Furthermore, Africa is the hottest of the tropical 'chimney' regions and also shows the greatest lightning activity. The land ocean contrast in boundary layer wet bulb potential temperature of 1–2 °C [7] does not translate to a land–ocean contrast in CAPE of 1000–2000 joule·kg^{-1} because of convective adjustment between land and sea. Further evidence for a primary role of dry bulb temperature in influencing global lightning has been found in comparisons of ionospheric potential and surface air temperature, in which dry bulb temperature correlations were stronger than those computed with wet bulb temperature (R. Markson and D. Boccippio, personal communication, 1999).

(ii) The evidence here for the greater survivability of boundary layer 'bubbles' with higher cloud base, with a lesser role for the magnitude of CAPE, are both consistent with recent empirical findings on global thunderstorm activity [51]. This recent study concluded that changes in global lightning on both the diurnal and the annual time scales were dominated by changes in the number of thunderstorms (rather than by changes in the mean flash rate per storm). The process postulated here provides for a larger number of storms in warmer conditions by providing for larger parcels that are more likely to attain thunderstorm status.

8. Conclusions

The weight of the evidence favors the traditional thermal hypothesis as the primary explanation for the land–ocean contrast in lightning activity. In simplest terms: land lightning is dominant because land is hotter than ocean. Surface characteristics influence the dry stage of conditional instability and ultimately updraft strength of the moist stage that is of primary importance to cloud microphysics and electrification. The updraft strength over oceans is strongly diminished from parcel theory predictions by mixing most prevalent with smaller oceanic parcels.

The inferred regulatory role of the dry stage of convection in lightning activity makes dry bulb temperature the primary thermodynamic variable in the response of the global circuit to temperature.

Acknowledgements. This study was brought to completion as a result of the kind invitation from Dr. Anne Bondiou to attend the Paris Workshop on Thunderstorms in November, 2001. Valuable discussions on topics of convection and aerosol are gratefully acknowledged with Marcia Baker, Alan Betts, Rich Blakeslee, Dennis Boccippio, Andy Detwiler, Chris Fairall, Steve Goodman, Jorg Hacker, Peggy LeMone, Luiz Machado, Ralph Markson, Vadim Mushtak, Nilton Renno, Danny Rosenfeld, Mark Weber and Ed Zipser. The global maps with TRMM data would not have possible without the efficient assistance of Erich Stocker and John Kwaitkowski. Several MIT students – Karen Rothkin, Sunnia Lin, Carlos Labrada and Twiggy Chan – helped with the data organization and analysis. Work on Oceanic Convective Weather at MIT Lincoln Laboratory has been supported by the FAA (Gloria Kulesa and Pete Kirchoffer). Research on global lightning at MIT has been supported by NASA GSFC (Bob Adler) on Grant NAG5-9637 and by the Physical Meteorology Program at NSF (Rod Rogers) on Grant ATM-0003346.

References

[1] C.E.P. Brooks, The distribution of thunderstorms over the globe, Geophys. Mem. London 24 (1925) 147–164.
[2] F.J.W. Whipple, On the association of the diurnal variation of electric potential gradient in fine weather with the distribution of thunderstorms over the globe, Quart. J. Roy. Met. Soc. 55 (1929) 1–17.
[3] E.T. Pierce, Some topics in atmospheric electricity, in: L.G. Smith (Ed.), Recent Advances in Atmospheric Electricity, Pergamon Press, 1958, pp. 5–16.
[4] R.E. Orville, R.W. Henderson, The global distribution of midnight lightning: December 1977 to August 1978, Mon. Wea. Rev. 114 (1986) 2640–2653.
[5] H.J. Christian, et al., The lightning imaging sensor, in: Proceedings 11th Int. Conf. on Atmospheric Electricity, Guntersville, AL, NASA/CP-1999-209261, 1999, pp. 746–749.
[6] E.R. Williams, S.J. Heckman, The local diurnal variation of cloud electrification and the global diurnal variation of negative charge on the earth, J. Geophys. Res. 98 (1993) 5221–5234.
[7] E.R. Williams, N.O. Renno, An analysis of the conditional instability of the tropical atmosphere 121 (1993) 21–36.
[8] E.R. Williams, The Schumann resonance: a global tropical thermometer, Science 256 (1992) 1184–1187.
[9] E.R. Williams, Global circuit response to seasonal variations in global surface air temperature, Mon. Wea. Rev. 122 (1994) 1917–1929.
[10] E.R. Williams, Global circuit response to temperature on distinct time scales: A status report, in: M. Hayakawa (Ed.), Atmospheric and Ionospheric Phenomena Associated with Earthquakes, Terra Scientific, Tokyo, 1999.
[11] C. Price, Global surface temperatures and the atmospheric electric circuit, Geophys. Res. Lett. 20 (1993) 1363.
[12] M. Fullekrug, A. Fraser-Smith, Global lightning and climate variability inferred from ELF field variations, Geophys. Res. Lett. 24 (1998) 2411–2414.
[13] N. Reeve, R. Toumi, Lightning activity as an indicator of climate change, Quart. J. Roy. Met. Soc. 125 (1999) 893–903.
[14] R. Markson, C. Price, Ionospheric potential as a proxy index for global temperature, Atmos. Res. 51 (1999) 309–314.
[15] A. Gettelman, D.J. Seidel, M.C. Wheeler, R.J. Ross, Multi-decadal trends in tropical convective available potential energy, J. Geophys. Res., 2002, in press.
[16] C. Lucas, M.A. LeMone, E.J. Zipser, Reply to Michaud, L.M., Comment on “Convective available potential energy in the environment of oceanic and continental clouds”, J. Atmos. Sci. 53 (1996) 1212–1214.
[17] J. Halverson, T. Rickenbach, B. Roy, H. Pierce, E. Williams, Environmental characteristics of convective systems during TRMM-LBA, Mon. Wea. Rev. 130 (2002) 1493–1509.

[18] F.-M. Breon, D. Tanre, S. Generoso, Aerosol effect on cloud droplet size monitored by satellite, Science 295 (2002) 834–838.
[19] E.R. Williams, et al., Contrasting convective regimes over the Amazon: Implications for cloud electrification, J. Geophys. Res., 2002, in press.
[20] R.E. Orville, G.R. Huffines, J. Nielsen-Gammon, R. Zhang, B. Ely, S. Steiger, S. Phillips, S. Allen, W. Read, Enhancement of cloud-to-ground lightning over Houston, Texas, Geophys. Res. Lett. 28 (2001) 2597–2600.
[21] F.H. Ludlam, Clouds and Storms: The Behavior and Effect of Water in the Atmosphere, Pennsylvania State University Press, 1980.
[22] W.R. Cotton, R.A. Anthes, Storm and Cloud Dynamics, Academic Press, 1989.
[23] H.R. Byers, R.R. Braham, The thunderstorm project, U.S. Weather Bureau, U.S. Dept. of Commerce, Washington, DC, 1949.
[24] M.A. LeMone, E.J. Zipser, Cumulonimbus vertical velocity events in GATE. Part I: Diameter, intensity and mass flux, J. Atmos. Sci. 37 (1980) 2444–2457.
[25] WMO, World distribution of thunderstorm days, WMO/OMM, No. 21.TP. 21, Parts I and II, 1956.
[26] E.R. Williams, The electrification of severe storms, in: C.A. Doswell III (Ed.), Severe Convective Storms, American Meteorological Society, 2001, pp. 527–561.
[27] E. Williams, S. Rutledge, S. Geotis, N. Renno, E. Rasmussen, T. Rickenback, A radar and electrical study of tropical 'hot towers', J. Atmos. Sci. 49 (1992) 1386–1395.
[28] M.B. Baker, H.J. Christian, J. Latham, A computational study of the relationships linking lightning frequency and other thundercloud parameters, Quart. J. Roy. Met. Soc. 121 (1995) 1525–1548.
[29] M.B. Baker, A.M. Blyth, H.J. Christian, J. Latham, K.L. Miller, A.M. Gadian, Relationships between lightning activity and various thundercloud parameters: Satellite and modeling studies, Atmos. Res. 51 (1999) 221–236.
[30] A. Hogan, Meteorological variation of maritime aerosols, in: A.F. Roddy, P.C. O'Connor (Eds.), Atmospheric Aerosols and Nuclei, Galway University Press, Galway, Ireland, 1977, pp. 503–507.
[31] D.P. Jorgenson, M.A. LeMone, Vertical velocity characteristics of oceanic convection, J. Atmos. Sci. 46 (1989) 621–640.
[32] C. Lucas, E. Zipser, M. LeMone, Vertical velocity in oceanic convection off tropical Australia, J. Atmos. Sci. 51 (1994) 3183–3193.
[33] G. Barnes, Severe local storms in the tropics, in: C.A. Doswell III (Ed.), Severe Convective Storms, Meteorological Monographs, American Meteorological Society, 2001, pp. 359–432.
[34] E.J. Zipser, Some views on 'hot towers' after 50 years of tropical field programs and two years of TRMM data, in: Meteorological Monographs, American Meteorological Society, 2002, in press.
[35] B.A. Wielicki, R.M. Welch, Cumulus cloud properties derived using Landsat satellite data, J. Clim. Appl. Met. 25 (1986) 261–276.
[36] S. Rutledge, E. Williams, T. Keenan, The Down Under Doppler and Electricity Experiment (DUNDEE): Overview and preliminary results, Bull. Am. Met. Soc. 73 (1992) 3–16.
[37] A.H. Woodcock, Soaring over the open sea, Scientific Monthly 55 (1942) 1–7.
[38] M. Bottomley, C.K. Folland, J. Hsuing, R.E. Newell, D.E. Parker, Global Ocean Surface Temperature Atlas, UK Met. Office and Massachusetts Institute of Technology, 1990.
[39] A.K. Betts, The parameterization of deep convection, in: R.K. Smith (Ed.), The Physics and Parameterization of Moist Atmospheric Convection, in: NATO ASI Series C, Vol. 505, Kluwer Academic, Dordrecht, 1997, pp. 255–279.
[40] B.R. Morton, G.I. Taylor, J.S. Turner, Turbulent gravitational convection for maintained and instantaneous sources, Proc. Roy. Soc. London A 234 (1956) 1–23.
[41] A.G. Williams, J.M. Hacker, The composite shape and structure of coherent eddies in the convective boundary layer, Boundary-Layer Meteor. 61 (1992) 213–245.
[42] H. Johari, Mixing in thermals with and without buoyancy reversal, J. Atmos. Sci. 49 (1992) 1412–1426.
[43] T.G. Kyle, W.R. Sand, D.J. Musil, Fitting measurements of thunderstorm updraft profiles to model profiles, Mon. Wea. Rev. 104 (1976) 611–617.
[44] C.A. Doswell III, Severe Convective Storms, in: Meteorological Monographs, Vol. 28, American Meteorological Society, November 2001.
[45] H. Riehl, J.S. Malkus, On the heat balance in the equatorial trough zone, Geophysica 6 (1958) 503–538.
[46] D. Henning, Atlas of the Surface Heat Balance of the Continents, Gebrider Bortraeger, Berlin, 1989.
[47] M.I. Budyko, The Evolution of the Biosphere, Reidel, 1986.
[48] E.W. McCaul Jr., C. Cohen, The impact of simulated storm structure and intensity on variations in the mixed layer and moist layer depths, Mon. Wea. Rev. 130 (2002) 1722–1748.
[49] E.R. Toracinta, D.J. Cecil, E.J. Zipser, S.W. Nesbitt, Radar, passive microwave and lightning characteristics of precipitating systems in the tropics, Mon. Wea. Rev. 130 (2002) 802–824.

[50] E.R. Jayaratne, Conditional instability and lightning activity in Gabarone, Botswana, Meteorol. Atmos. Phys. 62 (1993) 169–175.
[51] E. Williams, K. Rothkin, D. Stevenson, D. Boccippio, Global lightning variations caused by changes in thunderstorm flash rate and by changes in the number of thunderstorms, J. Appl. Met. 39 (2000) 2223–2230.
[52] S.J. Goodman, D.J. Cecil, Structure and characteristics of precipitation systems observed by TRMM, Preprints, in: 11th Conf. On Satellite Meteorology and Oceanography, 15–18 October, Madison, WI, American Meteorological Society, Boston, 2001, pp. 464–467.